

Photoproduction of $\gamma N \rightarrow K^+\Sigma^*(1385)$ in the Reggeized framework

Byung-Geel Yu^{1,*} and Kook-Jin Kong^{1,†}

¹*Research Institute of Basic Sciences, Korea Aerospace University, Goyang, 412-791, Korea*

Photoproduction of $K\Sigma^*(1385)$ on the nucleon is investigated within the Regge framework and the reaction mechanism is analyzed based on the data existing in the channels $\gamma p \rightarrow K^+\Sigma^{*0}$ and $\gamma n \rightarrow K^+\Sigma^{*-}$. The Reggeization of the t -channel meson exchanges $K(494) + K^*(892) + K_2^*(1430)$ is employed to construct the photoproduction amplitude. The Rarita-Schwinger formalism is applied for the spin-3/2⁺ strangeness-baryon Σ^* with a special gauge prescription utilized for the convergence of these reaction processes. Within a set of coupling constants determined from the symmetry argument for the K and K^* and from the duality and vector dominance for the K_2^* , the data of the both processes are reproduced to a good degree. The production mechanism of these processes are featured by the dominance of the contact term plus the K exchange with the role of the K_2^* following rather than the K^* .

PACS numbers: 25.20.Lj, 11.55.Jy, 13.60.Rj, 13.60.Le, 14.40.Df

I. INTRODUCTION

Kaon photoproduction off the nucleon target has been a useful tool to investigate strangeness production with data on a clean background from the electromagnetic probe. The experimental studies of the reactions involving $\Lambda(1116)$, and $\Sigma(1190)$ hyperons, or their resonances in the final state have been extensively conducted up to recent at the electron/photon accelerator for hadron facilities [1–4].

Of recent experimental achievements on these reactions the measurements of reaction cross sections for the $\gamma p \rightarrow K^+\Sigma^{*0}(1385)$ process from the CLAS [4, 5] and LEPS [6], and the $\gamma n \rightarrow K^+\Sigma^{*-}(1385)$ process from the LEPS [7] Collaboration draw our attention. In these reactions One reason for our interest is an advantage of studying baryon resonances whose existences have been predicted by the quark model, but are still missing, or remain an indefinite state. On the other hand, these reactions have their own issues of how to deal with the spin-3/2 baryon resonance in describing the reaction, because the propagation of the spin-3/2 resonance would give rise to a divergence as the reaction energy increases [8, 9].

Theoretical investigation of baryon resonances in the $\gamma p \rightarrow K^+\Sigma^{*0}$ process was carried out in Ref. [10], where a set of Δ and N^* resonances was considered in the effective Lagrangian approach. In this pioneering work the role of the baryon resonances was analyzed up to spin-5/2 state in the s - and u -channel contributions to the reaction process. Meanwhile, as an extension to the high energy realm a Regge plus resonance approach was applied for the $\gamma p \rightarrow K^+\Sigma^{*0}$ and $\gamma n \rightarrow K^+\Sigma^{*-}$ processes in Refs. [11, 12] with the empirical data up-dated by the recent experiments. However, in these works, the description of the reactions was complicated by using a

hybrid-type propagation which mixed the pure Regge pole and the Feynman propagator in the t -channel, apart from the cutoff functions to suppress the divergence at high energies, as in Ref. [10].

In this paper, we investigate photoproduction of $K\Sigma^*$ in two different isospin channels, $\gamma p \rightarrow K^+\Sigma^{*0}$ and $\gamma n \rightarrow K^+\Sigma^{*-}$, where the Reggeization of the t -channel meson exchange is exploited for the photoproduction amplitude at forward angles and high energies. Our focus here is to describe these reaction processes up to high energy without fit-parameters rather than to search for baryon resonances, because their roles in these reactions are found to be less important as discussed in Ref. [10]. Avoiding such complications as mentioned above, we will utilize the model of the $\gamma N \rightarrow \pi^\pm\Delta$ in Ref. [8] to apply to the present processes with the coupling constant $f_{KN\Sigma^*}$ considered from the SU(3) symmetry. Since the Σ^* of 3/2⁺ is the lowest mass hyperon in the baryon decuplet, this will be a valuable test of the flavor SU(3) symmetry with an expectation that the production mechanism of $K\Sigma^*$ is essentially identical to the $\pi\Delta$ case.

For the analysis of the process involving the spin-3/2 baryon resonance, in particular, it is worth asking how to describe the process without cutoff functions because they could sometimes hide the pieces of the reaction mechanism that are missing, or malfunctioning through the adjustment of the cutoff masses. From the previous studies on photoproduction of $\pi\Delta$ [8] we have learned two important things as to the dynamical feature of the spin-3/2 baryon photoproduction: The minimal gauge prescription is the one requisite for a convergence of the reaction cross section and the other is the role of the tensor meson $a_2(1320)$ significant in the high energy region. Therefore, as a natural extension of the model in Ref. [8] to strangeness sector, we here consider the $K(494) + K^*(892) + K_2^*(1430)$ exchanges in the t -channel to analyze the production mechanism of the $\gamma p \rightarrow K^+\Sigma^{*0}$ and $\gamma n \rightarrow K^+\Sigma^{*-}$ processes.

This paper is organized as follows. In Sec. II, we discuss the construction of the photoproduction amplitude in association with the gauge-invariant K exchange in

* E-mail: bgyu@kau.ac.kr

† E-mail: kong@kau.ac.kr

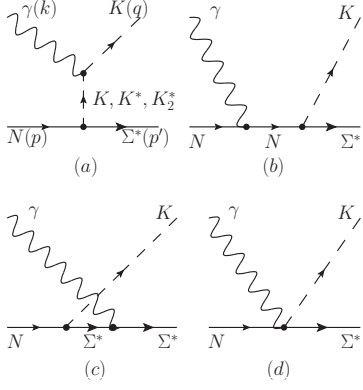


FIG. 1. Feynman diagrams for $\gamma N \rightarrow K^+ \Sigma^*$. The exchange of K in the t -channel (a), the proton-pole in the s -channel (b), the Σ^* -pole in the u -channel (c), and the contact term (d) are the basic ingredients for gauge invariance of the reaction. The K^* and K_2^* exchanged in the t -channel (a) are themselves gauge-invariant.

the t -channel. This will include a brief introduction of the minimal gauge, and the new coupling vertex for the tensor meson interaction $K_2^* N \Sigma^*$ which has been missed in previous works. Numerical results in the total and differential cross sections as well as the beam polarization asymmetry are presented for both reactions in Sec. III. We give a summary and discussion in Sec. IV. The SU(3) coefficients for the octet and decuplet baryons coupling to octet mesons are given in the Appendix.

II. FORMALISM

For a description of the reaction,

$$\gamma(k) + N(p) \rightarrow K(q) + \Sigma^*(p'), \quad (1)$$

with the momenta of the initial photon, nucleon and the final K and Σ^* denoted by k , p , q , and p' , respectively, we first construct the photoproduction amplitude which is gauge invariant as to the coupling of photon with particles in the reaction process. Then, the Reggeization of the t -channel meson-pole follows as has been done before.

A. Photoproduction amplitude

Viewed from the t -channel meson exchange the Born amplitudes in four different isospin channels are read as

$$M_{\gamma p \rightarrow K^+ \Sigma^{*0}} = M_K + M_{K^*} + M_{K_2^*}, \quad (2)$$

$$M_{\gamma n \rightarrow K^+ \Sigma^{*-}} = \sqrt{2} (M_K + M_{K^*} + M_{K_2^*}), \quad (3)$$

$$M_{\gamma p \rightarrow K^0 \Sigma^{*+}} = -\sqrt{2} (M_{K^*} + M_{K_2^*}), \quad (4)$$

$$M_{\gamma n \rightarrow K^0 \Sigma^{*0}} = - (M_{K^*} + M_{K_2^*}), \quad (5)$$

where the $\sqrt{2}$ factors and signs result from our convention of the meson-baryon-decuplet coupling of the $10 - 8 - 8$ type presented in the Appendix. Hereafter, we call the reaction process in Eq. (2), the γp process, and the process in Eq. (3), the γn process, respectively.

In experimental sides, the cross sections for total and differential were measured recently for the charged state Eq. (2) at the CLAS [4] and LEPS [6] Collaborations, and the differential cross section and the beam asymmetry were measured for the process in Eq. (3) at the LEPS Collaboration [7]. There exist data from the CBCG [13] and ABBHBM Collaboration [14, 15] in the pre-1970's where the total cross section for the charged process in Eq. (2) as well as the total and differential cross sections for the process in Eq. (3) reported by the ABHBM Collaboration [16]. Therefore, these data will be of use to constrain the physical quantities such as the coupling constants in the reaction once the trajectories of the Regge-poles for K , K^* , and K_2^* are chosen.

B. $K(494)$ exchange

For nucleon, kaon, and Σ^* charges, the current conservation following the charge conservation, $e_N - e_K - e_{\Sigma^*} = 0$, requires that the γp process includes the proton-pole in the s -channel and the contact term for gauge-invariance of the t -channel K exchange. Similarly the γn process includes the u -channel Σ^* -pole and the contact term in addition to the K exchange, respectively. These are depicted in Fig. 1. Thus, the gauge-invariant K exchange in the t -channel for these reactions are given by

$$iM_K^{\gamma p} = \bar{u}_\nu(p') i \left[M_{t(K)}^{\nu\mu} + M_{s(N)}^{\nu\mu} + M_c^{\nu\mu} \right] \epsilon_\mu(k) u(p), \quad (6)$$

$$iM_K^{\gamma n} = \bar{u}_\nu(p') i \left[M_{t(K)}^{\nu\mu} + M_{u(\Sigma^*)}^{\nu\mu} + M_c^{\nu\mu} \right] \epsilon_\mu(k) u(p), \quad (7)$$

where

$$iM_{s(N)}^{\nu\mu} = \Gamma_{KN\Sigma^*}^\nu(q) \frac{\not{p} + \not{k} + M_N}{s - M_N^2} \Gamma_{\gamma NN}^\mu(k), \quad (8)$$

$$iM_{t(K)}^{\nu\mu} = \Gamma_{\gamma KK}^\mu(q, Q) \frac{1}{t - m_K^2} \Gamma_{KN\Sigma^*}^\nu(Q), \quad (9)$$

$$iM_{u(\Sigma^*)}^{\nu\mu} = \Gamma_{\gamma \Sigma^* \Sigma^*}^{\nu\mu\sigma}(k) \frac{\not{p}' - \not{k} + M_{\Sigma^*}}{u - M_{\Sigma^*}^2} \Pi_{\sigma\beta}^{\Sigma^*}(p' - k) \times \Gamma_{KN\Sigma^*}^\beta(q), \quad (10)$$

with $Q^\mu = (q - k)^\mu$, the t -channel momentum transfer, and the spin-3/2 projection which is given by

$$\Pi_{\Sigma^*}^{\mu\nu}(p) = -g^{\mu\nu} + \frac{\gamma^\mu \gamma^\nu}{3} + \frac{\gamma^\mu p^\nu - \gamma^\nu p^\mu}{3M_{\Sigma^*}^2} + \frac{2p^\mu p^\nu}{3M_{\Sigma^*}^2}. \quad (11)$$

Here $u_\nu(p')$, $u(p)$, and $\epsilon_\mu(k)$ are the spin-3/2 Rarita-Schwinger field for the $\Sigma^*(1385)$, Dirac spinor for nucleon, and the spin polarization of photon, respectively.

The charge-coupling vertices γNN , $\gamma \Sigma^* \Sigma^*$ and γKK [8] are given as follows,

$$\epsilon_\mu \Gamma_{\gamma NN}^\mu = e_N \not{\epsilon}, \quad (12)$$

$$\epsilon_\mu \Gamma_{\gamma \Sigma^* \Sigma^*}^{\nu\mu\sigma} = -e_{\Sigma^*} (g^{\nu\sigma} \not{\epsilon} - \epsilon^\nu \gamma^\sigma - \gamma^\nu \epsilon^\sigma + \gamma^\nu \not{\epsilon} \gamma^\sigma), \quad (13)$$

$$\epsilon_\mu \Gamma_{\gamma KK}^\mu(q, Q) = e_K (q + Q)^\mu \epsilon_\mu, \quad (14)$$

where e_N , e_{Σ^*} , and e_K are the nucleon, Σ^* and kaon charges, respectively.

For the strong coupling vertex $KN\Sigma^*$ we use

$$\Gamma_{KN\Sigma^*}^\nu(q) = \frac{f_{KN\Sigma^*}}{m_K} q^\nu, \quad (15)$$

and neglect the off-shell effect of the spin-3/2 Rarita-Schwinger field for simplicity. Then, the contact term is given by

$$iM_c^{\nu\mu} = -e_K \frac{f_{KN\Sigma^*}}{m_K} g^{\nu\mu}. \quad (16)$$

Note that the charge-coupling terms in Eqs. (12), (13), and (14) satisfy the Ward identities in their respective vertices [8], and the full expressions for the spin-3/2 baryon electromagnetic form factors will be found in Ref. [9].

Since the mass of Σ^* lies below $\bar{K}N$ threshold the empirical decay channel $\Sigma \rightarrow \bar{K}N$ is not available for the estimate of the $KN\Sigma^*$ coupling constant, and we follow the SU(3) symmetry which predicts,

$$\frac{f_{\pi^- p \Delta^{++}}}{m_\pi} = -\sqrt{6} \frac{f_{K^+ p \Sigma^{*0}}}{m_K}, \quad (17)$$

and determine the coupling constant $f_{K^+ p \Sigma^{*0}}$ from the empirically known coupling constant $f_{\pi^- p \Delta^{++}}$. (See the Clebsch-Gordan coefficients with phase for the SU(3) baryon decuplet in the Appendix.) Hereafter, we will write $f_{K^+ p \Sigma^{*0}}$ as $f_{KN\Sigma^*}$ for brevity. In our previous work [8] we considered the coupling constant in the range from $f_{\pi^- p \Delta^{++}} = 1.7$ to 2. From these we estimate $f_{KN\Sigma^*} = -2.46$ and -2.83 , respectively. In other model calculations, however, the determination of $f_{KN\Sigma^*}$ is found to be rather scattered, e. g., $f_{KN\Sigma^*} = -3.22$ for the γp process in the effective Lagrangian approach by applying $f_{\pi^- p \Delta^{++}} = 2.23$ to the symmetry relation above [10]. The coupling constant $f_{KN\Sigma^*} = -4.74$ for the γp process [11], and -1.22 for the γn process [12] were obtained from the χ^2 -fit of data in the Regge plus resonance approach. In this work we take the coupling constant $f_{KN\Sigma^*} = -2.2$ within the range discussed above for a better agreement with experiment.

Minimal gauge

It is well known that the propagation of spin-3/2 Σ^* baryon in Eq. (10) causes divergence of the reaction at high energy. However, if we expect that only the peripheral K exchange in the t -channel should dominate at high

energies and small angles, then the particle exchanges in the reaction should contribute only to the Coulomb component of the photoproduction currents in Eqs. (6) and (7). This we call the minimal gauge prescription for the K exchange advocated in Refs. [8, 17, 18], and this is physically sensible because the higher multipoles of the Σ^* as a resonance are defined uniquely in the static limit and such a uniqueness can no longer be valid at high energy.

In the Reggeized model we recall that the u -channel Σ^* -pole in Eq. (7) as well as the s -channel proton-pole term in Eq. (6) is introduced merely to preserve gauge invariance for the t -channel K -pole exchange, respectively. By the above speculation at high energies we consider only the Coulomb components of the s -, and u -channel amplitudes that are indispensable to restore gauge invariance of the K exchange. Technically speaking, these correspond to the non-gauge invariant terms in the s - and u -channels after we remove the transverse component of the production current by redundancy with respect to gauge invariance.

In the u -channel amplitude in Eq. (10), for instance, the full expression is now written as [8],

$$iM_{u(\Sigma^*)} = e_{\Sigma^*} \frac{f_{KN\Sigma^*}}{m_K} \bar{u}^\nu(p') \left[\frac{2\epsilon \cdot p'}{u - M_{\Sigma^*}^2} g_{\nu\alpha} + G_{\nu\alpha}(p', k) \right] q^\alpha u(p), \quad (18)$$

where $G_{\nu\alpha}(p', k)$ is the part of the amplitude which collects all the terms that are gauge-invariant themselves. Thus, in this minimal gauge the production amplitude simply consists of the non-invariant terms in three channels, i.e.,

$$iM_K = \frac{f_{KN\Sigma^*}}{m_K} \bar{u}_\nu(p') \left[q^\nu \frac{2p \cdot \epsilon}{s - M_N^2} e_N + e_{\Sigma^*} \frac{2p' \cdot \epsilon}{u - M_{\Sigma^*}^2} q^\nu + e_K \frac{2q \cdot \epsilon}{t - m_K^2} (q - k)^\nu \right] u + iM_c. \quad (19)$$

With the K exchange given in Eq. (19), we now make it Reggeized by the following procedure,

$$\mathcal{M}_K = M_K \times (t - m_K^2) \mathcal{R}^K(s, t), \quad (20)$$

where

$$\mathcal{R}^\varphi = \frac{\pi \alpha'_\varphi}{\Gamma(\alpha_\varphi(t) + 1 - J) \sin \pi \alpha_\varphi(t)} \left(\frac{s}{s_0} \right)^{\alpha_\varphi(t) - J}, \quad (21)$$

is the Regge pole written collectively for the meson $\varphi (= K, K^*, K_2^*)$ of spin- J with the canonical phase $\frac{1}{2}((-1)^J + e^{-i\pi\alpha_\varphi(t)})$ taken for the exchange-nondegenerate meson in general.

For the trajectory of K we use

$$\alpha_K(t) = 0.7(t - m_K^2). \quad (22)$$

The phases of the K exchange is taken from the reaction $\gamma p \rightarrow K^+ \Lambda$ [19] as a natural extension. As for the $\gamma n \rightarrow K^+ \Sigma^-$ process, however, we favor to choose the phase of the K exchange for a better description of the reaction processes, as will be discussed later.

C. $K^*(892)$ exchange

The K^* exchange in the t -channel is one of the ingredients to consider for the analysis of the production mechanism.

The production amplitude is given by [9],

$$i\mathcal{M}_{K^*} = -i \frac{g_{\gamma K K^*}}{m_0} \epsilon^{\mu\rho\lambda\alpha} \epsilon_{\mu k\rho q\lambda} \bar{u}_\nu(p') \times (-g_{\alpha\beta} + Q_\alpha Q_\beta / m_{K^*}^2) \Gamma_{K^* N \Sigma^*}^{\beta\nu}(Q, p', p) u(p) \times \mathcal{R}^{K^*}(s, t). \quad (23)$$

For the $K^* N \Sigma^*$ coupling we consider only the following form,

$$\Gamma_{K^* N \Sigma^*}^{\beta\nu}(q, p', p) = \frac{f_{K^* N \Sigma^*}}{m_{K^*}} (q^\beta \gamma^\nu - \not{q} g^{\beta\nu}) \gamma_5, \quad (24)$$

and disregard the other nonleading terms simply because the leading contribution of the K^* exchange in Eq. (24) itself is not significant. In our previous work on the $\gamma p \rightarrow \pi^\pm \Delta$ process we used $f_{\rho N \Delta} = 5.5$ for the Model I, and 8.57 for the Model II [9]. These values lead to $f_{K^* N \Sigma^*} = -2.58$ and -4.03 , respectively, according to the SU(3) relation

$$\frac{f_{\rho N \Delta}}{m_\rho} = -\sqrt{6} \frac{f_{K^* N \Sigma^*}}{m_{K^*}}. \quad (25)$$

With these values we try to find which one yields the better result in the numerical analysis. From the decay width $\Gamma_{K^* \rightarrow K \gamma} = 50$ keV for the charged state, we estimate $g_{\gamma K^* K} = \pm 0.254$ and take the negative sign for an agreement with data.

The trajectory for K^* is taken to be

$$\alpha_{K^*}(t) = 0.83t + 0.25, \quad (26)$$

which is consistent with the previous works [19, 20]. The complex phase for the γp and the constant phase for γn processes are considered for the exchange-degenerate (EXD) pair $K^*-K_2^*$.

D. $K_2^*(1430)$ exchange

It is found that the tensor-meson $a_2(1320)$ of spin-2 exchange plays the role at high energy from the previous studies of the reactions $\gamma N \rightarrow \pi^\pm N$ [21] and $\gamma N \rightarrow \pi^\pm \Delta$ [8]. Furthermore the role of the K_2^* in the strangeness sector is also noticeable in the $\gamma p \rightarrow K^+ \Lambda$ [19]. Therefore, it is quite reasonable to consider the tensor meson K_2^* exchange in these reaction processes. As an application of the $a_2 N \Delta$ coupling in Ref. [8] to the strangeness sector, we write the Lagrangian for the $K_2^* N \Sigma^*$ as,

$$\mathcal{L}_{K_2^* N \Sigma^*} = i \frac{f_{K_2^* N \Sigma^*}}{m_{K_2^*}} \bar{\Sigma}^{*\lambda} (g_{\lambda\mu} \partial_\nu + g_{\lambda\nu} \partial_\mu) \gamma_5 N K_2^{*\mu\nu}. \quad (27)$$

TABLE I. Physical constants from the SU(3) symmetry, Regge trajectories and phases for $^{(a)}\gamma p \rightarrow K^+ \Sigma^{*0}$ and $^{(b)}\gamma n \rightarrow K^+ \Sigma^{*-}$. The radiative decay constants are $g_{\gamma K K^*} = -0.254$ and $g_{\gamma K K_2^*} = 0.276$.

Meson	$^{(a)}$ Phase	$^{(b)}$ Phase	Cpl. const.
K	$e^{-i\pi\alpha}$	$(1 + e^{-i\pi\alpha})/2$	$f_{K N \Sigma^*} = -2.2$
K^*	$e^{-i\pi\alpha}$	1	$f_{K^* N \Sigma^*} = -4.03$
K_2^*	$e^{-i\pi\alpha}$	1	Eq. (28)

Here $K_2^{*\mu\nu}$ is the tensor field of spin-2 with the coupling constant assumed to be

$$\frac{f_{K_2^* N \Sigma^*}}{m_{K_2^*}} \approx -3 \frac{f_{K^* N \Sigma^*}}{m_{K^*}} \quad (28)$$

by a simple extension to the strangeness sector from the ρ and a_2 meson case which is based on the duality and vector dominance [22, 23]. In the $\pi \Delta$ photoproduction the tensor meson- Δ baryon coupling constant determined by such a relation above yielded a reasonable result in the high energy region, as illustrated in Ref. [8].

The Lagrangian for the $\gamma K K_2^*$ coupling was investigated in Ref. [24] and given by

$$\mathcal{L}_{\gamma K K_2^*} = -i \frac{g_{\gamma K K_2^*}}{m_0^2} \tilde{F}_{\alpha\beta} (\partial^\alpha K_2^{*\beta\rho} - \partial^\beta K_2^{*\alpha\rho}) \partial_\rho K, \quad (29)$$

where $\tilde{F}_{\alpha\beta} = \frac{1}{2} \epsilon_{\mu\nu\alpha\beta} F^{\mu\nu}$ is the pseudotensor field of photon. The decay of the tensor meson K_2^* to $K \gamma$ is reported to be $\Gamma_{K_2^* \rightarrow K \gamma} = (0.24 \pm 0.05)$ MeV in the Particle Data Group (PDG) and we estimate $g_{\gamma K K_2^*} = 0.276$ [19] with the sign determined to agree with existing data.

The Reggeized amplitude for the K_2^* exchange is thus written as

$$i\mathcal{M}_{K_2^*} = -i \frac{2g_{\gamma K K_2^*}}{m_0^2} \frac{f_{K_2^* N \Sigma^*}}{m_{K_2^*}} \epsilon^{\alpha\beta\mu\lambda} \epsilon_{\mu k\lambda} Q_\alpha q_\rho \times \Pi_{K_2^*}^{\beta\rho;\sigma\xi}(Q) \bar{u}^\nu(p') (g_{\nu\sigma} P_\xi + g_{\nu\xi} P_\sigma) \gamma_5 u(p) \times \mathcal{R}^{K_2^*}(s, t), \quad (30)$$

where $P = (p + p')/2$ and the spin-2 projection is given by

$$\Pi_{K_2^*}^{\beta\rho;\sigma\xi}(Q) = \frac{1}{2} (\eta^{\beta\sigma} \eta^{\rho\xi} + \eta^{\beta\xi} \eta^{\rho\sigma}) - \frac{1}{3} \eta^{\beta\rho} \eta^{\sigma\xi} \quad (31)$$

with $\eta^{\beta\rho} = -g^{\beta\rho} + Q^\beta Q^\rho / m_{a_2}^2$.

For the K_2^* Regge-pole exchange we take the EXD phase $e^{-i\pi\alpha_{K_2^*}}$ for the γp and the constant phase for the γn processes, respectively, as discussed above, and choose the trajectory

$$\alpha_{K_2^*}(t) = 0.83(t - m_{K_2^*}^2) + 2, \quad (32)$$

to be consistent with Ref. [19].

In model calculations where the Regge-poles are employed to estimate physical observables the results in shape and magnitude are, in general, very sensitive to a

change of the phase as well as the trajectory. Therefore, it is of importance to choose the phase of K exchange which dominates over other meson exchanges. We take the complex phase for the K exchange in the γp process, as before. In the case of γn process, however, the choice of the constant phase leads to an overestimation of the total cross section in the resonance peak, while fixing the coupling constant $f_{K+n\Sigma^{*-}} = \sqrt{2}f_{K+p\Sigma^{*0}}$. Without altering the coupling constant, thus, we take the canonical phase which is more adaptive to describe the reaction processes.

In Table I we list the coupling constants and phases used for the calculation of the $\gamma p \rightarrow K^+\Sigma^{*0}$ and $\gamma n \rightarrow K^+\Sigma^{*-}$ reactions.

III. NUMERICAL RESULTS

In this section we present numerical consequences in the cross sections for the total, differential and beam polarization for the reactions $\gamma p \rightarrow K^+\Sigma^{*0}$ and $\gamma n \rightarrow K^+\Sigma^{*-}$.

A. $\gamma p \rightarrow K^+\Sigma^{*0}$

Given the production amplitudes in Eq. (2) with the coupling constants in Table I determined from the symmetry consideration, we calculate total and differential cross sections for $\gamma p \rightarrow K^+\Sigma^{*0}$ and present the result to compare with existing data. There is a discrepancy between the recent CLAS data and old ones measured in the pre-1970's by the CBCG [13] and ABBHHM Collaboration [14, 15]. The solid curve in Fig. 2 corresponds to the full calculation of the cross section with the coupling constants chosen to agree with the CLAS data, and the respective contributions of meson exchanges are displayed. As shown in the figure the production mechanism is solely understood as the dominating role of the contact term in Eq. (16) plus the pseudoscalar K exchange in Eq. (9), while the tensor meson K_2^* exchange in Eq. (30) gives a contribution gradually growing as the energy increases. The contribution of the vector meson K^* exchange in Eq. (23) is small and less significant than that of the tensor-meson K_2^* . That the K^* contribution is small and thus insignificant is consistent with the observation in other model calculations of the process [10], and confirms the validity of the leading $K^*N\Sigma^*$ interaction considered only for the K^* exchange.

The dependences of differential cross sections on the angle and energy are presented in Figs. 3. The slope of the CLAS data in the forward direction is reproduced to a degree in the panels (a), (b), and (c). The rise of the cross section data in the backward angle in (c) may signify the contributions of the baryon resonances. For the energy dependence of the differential cross section in (d) our prediction also agrees with the LEPS data as well.

B. $\gamma n \rightarrow K^+\Sigma^{*-}$

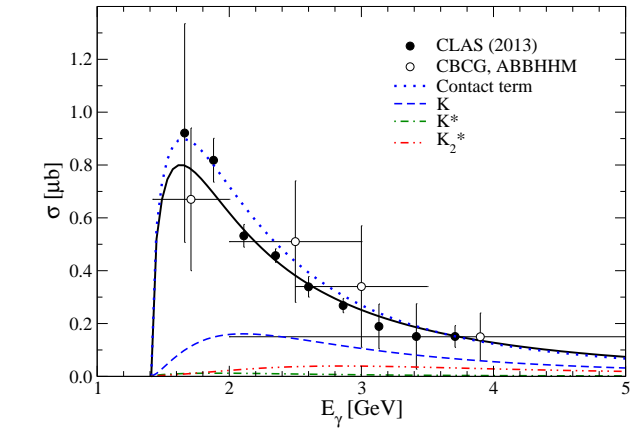


FIG. 2. Total cross section for $\gamma p \rightarrow K^+\Sigma^{*0}(1385)$. Contributions of the contact term and meson exchanges are shown in the dotted, dashed, dash-dotted and dash-dot-dotted curves, respectively. The dominance of the contact term is shown. The CLAS data are taken from Ref. [4]. The data of the CBCG and ABBHHM are from Refs. [13–15].

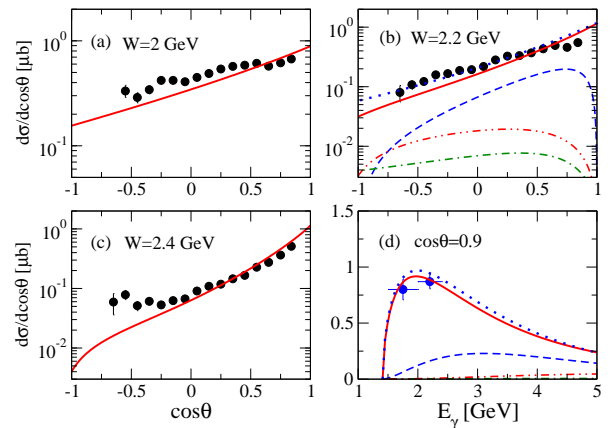


FIG. 3. Differential cross sections for $\gamma p \rightarrow K^+\Sigma^{*0}(1385)$. The angle dependence of the cross sections are shown in the first three panels (a), (b), (c) with the data taken from the CLAS Collaboration [4]. The energy dependence is shown in the panel (d) with data from the LEPS Collaboration [6]. The contributions of the contact terms and the respective meson exchanges are displayed in (b) and (d) with same notations as in Fig. 2.

The contributions of the contact term and the respective meson exchanges are analyzed in the panels (b) and (d).

There are various sorts of data on the $\gamma n \rightarrow K^+\Sigma^{*-}$ process in comparison to the former γp process. The total and differential cross sections are found in the experiment at the ABBHHM Collaboration in the mid-1970's [16]. Very recently the angular distribution and beam

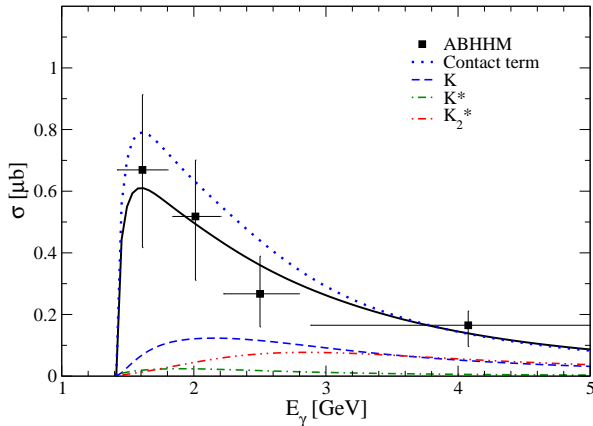


FIG. 4. Total cross section for $\gamma n \rightarrow K^+\Sigma^{*-}(1385)$. Contributions of the contact term and meson exchanges are displayed with the same notations as in Fig. 2. The dominance of the contact term is shown. Data are taken from Ref. [16].

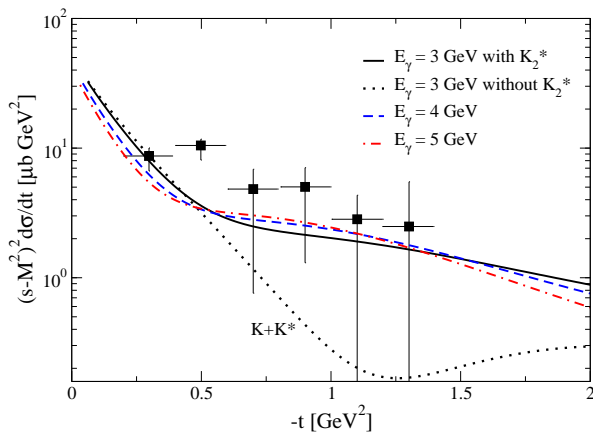


FIG. 5. Differential cross section $(s - M_n^2)^2 d\sigma/dt$ for $\gamma n \rightarrow K^+\Sigma^{*-}(1385)$ at $E_\gamma = 3, 4,$ and 5 GeV. The solid and dotted curves are the cross sections at $E_\gamma = 3$ GeV with and without K_2^* , showing the role of the tensor meson. Data are taken from Ref. [16].

polarization asymmetry were measured in the LEPS experiment [7].

We calculate the energy dependence of the cross section and present the result in Fig. 4. There might be a room for improving the accuracy in future experiment as can be seen in Fig. 2. But the data of the ABHHM are enough to test our model prediction at the present stage, exhibiting the maximum peak and the slope of the decrease along with the increase of photon energy. We note that the K_2^* exchange gives an equal amount of contribution to the K over $E_\gamma \approx 3$ GeV.

Figure 5 shows the differential cross section scaled by the factor $(s - M_n^2)^2$ so that the $-t$ distribution of the

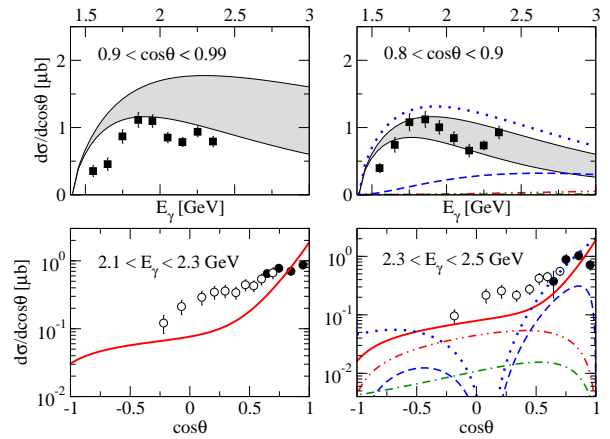


FIG. 6. Dependence of differential cross sections for $\gamma n \rightarrow K^+\Sigma^{*-}(1385)$ on the energy (upper panels) and angle (lower panels). Model predictions are given by the grey band to cover the range of angle denoted. The contributions of the contact terms and the respective meson exchanges estimated at $\cos\theta = 0.85$ are displayed in upper right and at $E_\gamma = 2.4$ GeV in the lower right panels with same notations as in Fig. 4. The dip structure appears there due to the canonical phase of the K exchange. Data of the LEPS (black squares) are taken from Ref. [7] and those of the CLAS (empty circles) are from Ref. [5].

cross section is energy independent. We reproduced the cross section at the photon energies, 3, 4, and 5 GeV up to the limit of the experiment, $E_\gamma = 5.3$ GeV. It should be pointed out that the role of the K_2^* is crucial to meet with the data in the region $-t > 0.5$ GeV^2/c^2 .

Shown in Fig. 6 is the energy dependence of the differential cross section at forward angles and its angle dependence in two energy bins. The energy dependence of the $d\sigma/d\cos\theta$ is shown in the range calculated between two boundaries $\cos\theta = 0.9$ and 0.99 in the first panel, for instance. The angle dependence of $d\sigma/d\cos\theta$ is calculated at the $E_\gamma = 2.2$ and 2.4 GeV, respectively. These results reproduce quite well the overall feature of the cross section data. The contributions of the contact terms and the respective meson exchanges are analyzed in upper right and lower right panels, where the dip structure of the K exchange, and of the contact term, as a result, are shown at the $-t \approx 0.3$ GeV^2 due to the zero of the trajectory $\alpha_K(t) = 0$ in the canonical phase of the K exchange.

The energy dependence of the beam polarization asymmetry Σ was measured in the LEPS experiment of the reaction $\gamma n \rightarrow K^+\Sigma^{*-}(1385)$ and the result is compared with the case of the $\gamma n \rightarrow K^+\Sigma^-(1190)$ in Fig. 7 in the same range of the angle, $0.6 < \cos\theta < 1$.

With the Σ defined as

$$\Sigma = \frac{d\sigma_y - d\sigma_x}{d\sigma_y + d\sigma_x}, \quad (33)$$

where $d\sigma_{x(y)} = \frac{d\sigma_{x(y)}}{d\Omega}$ is the component of the differential cross section in the xyz -system spanned by the photon

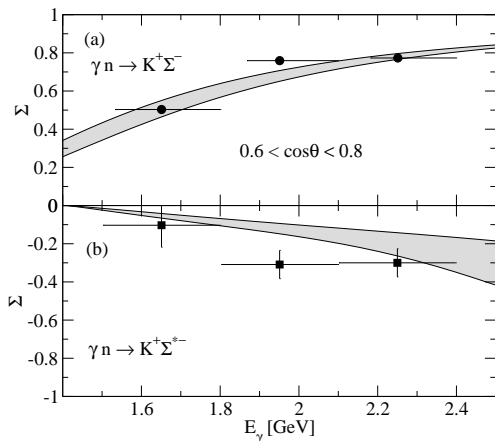


FIG. 7. Energy-dependence of beam polarization asymmetries for $\gamma n \rightarrow K^+\Sigma^-$ (1190) from $\Sigma = \frac{d\sigma_y - d\sigma_x}{d\sigma_y + d\sigma_x}$ (a) and $\gamma n \rightarrow K^+\Sigma^{*-}$ (1385) from $\Sigma = -\frac{d\sigma_y - d\sigma_x}{d\sigma_y + d\sigma_x}$ (b). The beam polarization asymmetry in (a) is calculated by the model in Ref. [19]. Model predictions are given by the grey band to cover the range of the angle denoted. Data are taken from Ref. [7].

momentum (z -direction) and two other axes orthogonal to it in the production plane, we calculated the Σ of the $\gamma p \rightarrow K^+\Sigma$ process in Fig. 7 (a) by using the model of Ref. [19] where the production amplitude consists of the $K + K^* + K_2^*$ similar to Eq. (3), but the phases for all the exchanged mesons are taken to be constant, i.e., 1. As for the case of the $\gamma n \rightarrow K^+\Sigma^{*-}$ process, however, the beam polarization Σ as shown by the grey band in Fig. 7 (b) is predicted in the present framework with the sign of the Σ in Eq. (33) reversed. At the present stage, we leave it a problem how to reconcile the sign of the Σ between theory and experiment, and suggest that such an uncertainty in measuring the Σ in the γn reaction needs to be more analyzed in future experiments.

IV. SUMMARY AND DISCUSSION

In this work, we have investigated the reaction processes $\gamma p \rightarrow K^+\Sigma^{*0}$ and $\gamma n \rightarrow K^+\Sigma^{*-}$ to analyze the production mechanism based on the data provided by the CLAS and LEPS Collaborations as well as those by the CBCG, ABBHBM, and ABHBM Collaborations. By using a set of coupling constants common in both reactions total and differential cross sections as well as the beam polarization asymmetry are analyzed and the results in these reactions are quite reasonable to account for the experimental data. Nevertheless, we need to work further on the beam polarization Σ to resolve the inconsistency between the model calculation and measurement.

The results obtained in this work show that the most important contribution comes from the contact term which is a feature of the spin-3/2 baryon photoproduction. Then, the contribution of the pseudoscalar K ex-

change follows as the dominant one among the t -channel meson exchanges. The role of the K^* exchange from the present analysis turned out to be of secondary importance, as concluded in previous works. Nevertheless, it cannot be neglected in these processes because of its relation with the K_2^* which plays the role crucial to explain the data at high energy, as demonstrated in the scaled differential cross section of the γn reaction.

A few remarks are in order. First, we note that the size of the total cross section for the γp process is about the same as that of the γn , though the amplitude of the latter process differs by a factor of $\sqrt{2}$ from the former, i.e.

$$\frac{\sigma_{\gamma n}}{\sigma_{\gamma p}} \sim \frac{|\sqrt{2}(\text{contact} + t\text{-ch. } K + \dots)|^2}{|\text{contact} + t\text{-ch. } K + \dots|^2} \sim 1. \quad (34)$$

This could be understood as the similar size of the contact term contribution which is dominant in both reactions, as shown in Figs. 2 and 4.

By comparing the maximum size of the cross section $\sigma \approx 10 \mu\text{b}$ for the $\gamma p \rightarrow \pi^+\Delta^0$ process [25] with that of $\sigma \approx 1$ for the $\gamma p \rightarrow K^+\Sigma^{*0}$ process, their ratio is basically consistent with the reduction of the leading coupling constant $f_{KN\Sigma^*}$ by a factor of 36 % as compared to the $f_{\pi N\Delta} = 1.7$ in the same mass unit, i.e.,

$$\frac{\sigma(\gamma p \rightarrow K^+\Sigma^{*0})}{\sigma(\gamma p \rightarrow \pi^+\Delta^0)} \approx \left| \frac{f_{KN\Sigma^*}}{f_{\pi N\Delta}} \right|^2. \quad (35)$$

Therefore, it is reasonable to assume that both reactions share the same production mechanism as the members of the baryon-decuplet within the present framework.

Finally, we give a comment on the study of N^* resonances, though it is beyond the scope of the present work. For future work it is desirable to investigate the role of N^* in the neutral processes such as in Eqs. (4) and (5), because they have only $K^* + K_2^*$ exchanges in the t -channel which are expected to be small as can be seen in Figs. 2 and 4. In this sense, the reaction $\gamma p \rightarrow K^0\Sigma^{*+}$ in Eq. (4), in particular, could provide a ground more advantageous to identify N^* resonances in the measured cross section of $\sigma = 0.68 \pm 0.48 (\mu\text{b})$ at $E_\gamma = 1.42 \sim 2$ GeV and $\sigma = 0.13 \pm 0.09 (\mu\text{b})$ at $E_\gamma = 2 \sim 5.8$ GeV [15], which is of the same order of magnitude as the charged ones we have presented in this work.

ACKNOWLEDGMENTS

We are grateful to Hungchong Kim for fruitful discussions. This work was supported by the grant NRF-2013R1A1A2010504 from National Research Foundation (NRF) of Korea.

Appendix A: SU(3) relation of the meson-baryon coupling constants for the interactions of the $\mathbf{8} - \mathbf{8} - \mathbf{8}$ and $\mathbf{10} - \mathbf{8} - \mathbf{8}$ types

We use the phase and coupling constants of the meson-baryon interaction (MBB) of the type $\mathbf{8} - \mathbf{8} - \mathbf{8}$ which is defined by the following tensor operators,

$$B_i^j = \begin{pmatrix} \frac{1}{\sqrt{2}}\Sigma^0 + \frac{1}{\sqrt{6}}\Lambda & \Sigma^+ & p \\ \Sigma^- & -\frac{1}{\sqrt{2}}\Sigma^0 + \frac{1}{\sqrt{6}}\Lambda & n \\ -\Xi^- & \Xi^0 & -\frac{2}{\sqrt{6}}\Lambda \end{pmatrix} \quad (\text{A1})$$

for the $J^P = \frac{1}{2}^+$ baryon octet, and

$$M_i^j = \begin{pmatrix} \frac{1}{\sqrt{2}}\pi^0 + \frac{1}{\sqrt{6}}\eta & \pi^+ & K^+ \\ \pi^- & -\frac{1}{\sqrt{2}}\pi^0 + \frac{1}{\sqrt{6}}\eta & K^0 \\ K^- & \bar{K}^0 & -\frac{2}{\sqrt{6}}\eta \end{pmatrix} \quad (\text{A2})$$

$$D^{111} = \Delta^{++}, \quad D^{112} = \frac{1}{\sqrt{3}}\Delta^+, \quad D^{122} = \frac{1}{\sqrt{3}}\Delta^0, \quad D^{222} = \Delta^-, \quad (\text{A4})$$

$$D^{113} = \frac{1}{\sqrt{3}}\Sigma^{*+}, \quad D^{123} = \frac{1}{\sqrt{6}}\Sigma^{*0}, \quad D^{223} = \frac{1}{\sqrt{3}}\Sigma^{*-}, \quad (\text{A5})$$

$$D^{133} = \frac{1}{\sqrt{3}}\Xi^{*0}, \quad D^{233} = \frac{1}{\sqrt{3}}\Xi^{*-}, \quad (\text{A6})$$

$$D^{333} = \Omega^{*-}. \quad (\text{A7})$$

The meson-baryon-decuplet baryon (MBD) interaction of the $\mathbf{10} - \mathbf{8} - \mathbf{8}$ type in SU(3) limit can be again from fully contracting the indices as

$$g\bar{D}^{ijk}B_j^l M_k^m \epsilon_{ilm} + \text{h.c.}, \quad (\text{A8})$$

where the Levi-Civita tensor ϵ_{ilm} is needed because the total number of index is odd. Therefore, only one type

for the $J^P = 0^-$ pseudoscalar meson octet.

The meson-baryon-baryon (MBB) interaction of the $\mathbf{8} - \mathbf{8} - \mathbf{8}$ type can be constructed from fully contracting the indices as

$$a\bar{B}_j^i B_k^j M_i^k + b\bar{B}_j^i B_i^k M_k^j + \text{h.c.}, \quad (\text{A3})$$

Therefore, two types of coupling are possible in the SU(3) limit, which are equivalent to the conventional F and D types.

For the $J^P = \frac{3}{2}^+$ baryon decuplet, totally symmetric tensor D^{ijk} can be identified with the baryon resonances.

of coupling is possible in the SU(3) limit as in Eq. (A8).

After a little algebra, the following relation is obtained;

$$\begin{aligned} \frac{f_{\pi^- p \Delta^{++}}}{m_\pi} &= -\sqrt{6} \frac{f_{K^+ p \Sigma^{*0}}}{m_K} = -\sqrt{3} \frac{f_{K^+ n \Sigma^{*-}}}{m_K} \\ &= \sqrt{3} \frac{f_{K^0 p \Sigma^{*+}}}{m_K} = \sqrt{6} \frac{f_{K^0 n \Sigma^{*0}}}{m_K}. \end{aligned} \quad (\text{A9})$$

-
- [1] M.E. McCracken *et al.*(CLAS Collaboration), Phys. Rev. C **81**, 025201 (2010).
[2] K.-H. Glander *et al.*, Eur. Phys. J. A **19**, 251 (2004).
[3] R. K. Bradford *et al.*(CLAS Collaboration), Phys. Rev. C **75**, 035205 (2007).
[4] K. Moriya *et al.*(CLAS Collaboration), Phys. Rev. C **88**, 045201 (2013).
[5] P. Mattione, Int. J. Mod. Phys. Conf. Ser. **26**, 1460101 (2014).
[6] M. Niiyama *et al.*(LEPS Collaboration), Phys. Rev. C **78**, 035202 (2008).
[7] K. Hicks *et al.*(LEPS Collaboration), Phys. Rev. Lett. **102**, 012501 (2009).
[8] B.-G. Yu and K.-J. Kong, arXiv:1611.09629 [hep-ph].
[9] B.-G. Yu and K.-J. Kong, arXiv:1612.02071 [hep-ph].
[10] Y. Oh, C. M. Ko, K. Nakayama, Phys. Rev. C **77**, 045204 (2008).
[11] Jun He, Phys. Rev. C **89**, 055204 (2014).
[12] X.-Y. Wang, J. He, H. Habertzettl, Phys. Rev. C **93**, 045204 (2016).
[13] J. H. R. Crouch *et al.*, Phys. Rev. **156**, 1426 (1967).
[14] R. Erbe *et al.*, Nuovo Cimento **49A**, 504 (1967).
[15] R. Erbe *et al.*, Phys. Rev. **188**, 2060 (1969).
[16] P. Benz *et al.*, Nucl. Phys. B **115**, 385 (1976).
[17] P. Stichel and M. Scholz, Nuovo Cimento **34**, 1381 (1964).
[18] J. A. Campbell, R. B. Clark and D. Horn, Phys. Rev. D **2**, 217 (1970).
[19] B. G. Yu, T. K. Choi and W. Kim, Phys. Lett. B **701** 332
[20] M. Guidal, J.-M. Laget, and M. Vanderhaeghen, Nucl. Phys. A **627**, 645 (1997).
[21] B. G. Yu, T. K. Choi and W. Kim, Phys. Rev. C **83**, 025208 (2011).
[22] G. Goldstein and J. F. Owens III, Nucl. Phys. B **71** 461 (1974).

- [23] R. L. Thews, Phys. Lett. B **65** 343 (1976).
[24] F. Giacosa, Th. Gutsche, V. E. Lyubovitskij, and A. Faessler, Phys. Rev. D **72**, 114201 (2005).
[25] C. Wu *et al.*, E. P. J. A **23**, 317 (2005).